Available online at http://scik.org
Commun. Math. Biol. Neurosci. 2026, 2026:11
https://doi.org/10.28919/cmbn/9640
ISSN: 2052-2541

OPTIMAL CONTROL ON MODEL OF COVID-19 WITH INEFFECTIVE VACCINATION AND QUARANTINE

MEHDI BOUZIANE[1], IQBAL H. JEBRIL[2], IQBAL M. BATIHA[2,3,*]

[1]Department Mathematics, Higher Normal School of Mostaganem, Mostaganem, Algeria

[2]Department of Mathematics, Al Zaytoonah University of Jordan, Amman 11733, Jordan

[3]Nonlinear Dynamics Research Center (NDRC), Ajman University, Ajman, United Arab Emirates

Abstract. In this paper, we present an optimal control approach for an (SEIRV) epidemic model of COVID-19 disease by controlling quarantine measures on susceptible individuals and controlling the vaccination rate for susceptible individuals, exposed but not yet infectious individuals, and asymptomatic infectious individuals to reduce the disease burden and related costs. We have proven that an optimal control does exist, and we used Pontryagin's maximum principle to characterize the optimal control. In numerical simulations, we solve the optimal control problem by the fourth-order Runge–Kutta method. Moreover, we discuss different cases for optimal control of quarantine measures and vaccination quantity presented through graphical representations.

Keywords: COVID-19; mathematical model; optimal control; Pontryagin's maximum principle.
2020 AMS Subject Classification: 49J15, 92D30, 34K20.

1. Introduction

In recent years, considerable attention has been devoted to the development of analytical and numerical techniques for solving classical and fractional differential equations arising in

*Corresponding author
E-mail address: i.batiha@zuj.edu.jo
Received October 14, 2025

applied sciences, particularly in epidemic and biomedical modeling. Various efficient algorithms have been proposed for Volterra integro-differential equations and fractional differential systems, highlighting their accuracy and computational efficiency [1, 2, 3]. Fractional-order modeling has also proved to be a powerful tool for capturing memory and hereditary effects in the transmission dynamics of infectious diseases, including Zika virus and COVID-19, as well as in control-oriented epidemic frameworks [4, 5, 6, 7]. More recently, fractional mathematical models have been successfully applied to emerging infectious diseases such as monkeypox and to biomedical applications including cancer progression, offering deeper insight into stability, control, and long-term behavior of complex dynamical systems [8, 9, 10, 11].

The world has been witnessing the spread of a new virus known as COVID-19 (Coronavirus disease 2019). This infectious disease originated in China in November 2019 and has quickly propagated to numerous countries globally [12], whereby by the end of March 2022, approximately 480 million confirmed cases of COVID-19 had been reported, and over 6 million deaths had occurred [13]. It is a pandemic impacting all age groups, with mortality rates rising with age, starting at 0.2% for 39-year-olds and reaching 14.8% for those over 80 [14]. In addition, common COVID-19 symptoms are fever, fatigue, dry cough, sore throat, headache, and breathing issues [15].

Efforts to control COVID-19 have focused on exploring various treatment options and developing multiple vaccines aimed at preventing and mitigating the impact of the virus [16, 17]. In addition, several preventive measures have proven effective. These include quarantine and isolation to limit contact with infected individuals, social distancing to reduce close interactions, wearing masks to prevent airborne spread, regular handwashing to remove potential viruses, and disinfecting surfaces to eliminate viral particles [18, 19]. These initiatives are crucial in managing the spread and severity of the disease, ultimately aiming to reduce the global health burden caused by the pandemic.

The urgent global task is to understand COVID-19 transmission and apply effective measures, such as vaccination and quarantine. These practices (preventive measures) have significant economic and social impacts for any country due to the high costs and logistical challenges involved, making universal vaccination and quarantine less viable options, leading to an increasing desire to relax them and identify the minimal level of contact reduction necessary to meet public health goals [20]. For this reason, many scientists employ optimal control theory to mathematically model and identify the most effective strategies for managing dynamic systems, assessing the efficiency and costs of various policies and control measures [21]. Lemecha et al. [22] developed a new COVID-19 epidemic model to identify optimal control strategies while taking into account control costs using optimal control theory. The author in [23] formulated an optimal control problem where the population engages in social distancing and the treatment of infected individuals serves as the control variable. By applying the Pontryagin maximum principle, the most effective control strategies were identified. The authors in [24] examined effective control measures and cost-effectiveness strategies to mitigate COVID-19 in a specific region. Khajanchi and Mondal [25] proposed an optimal control model for COVID-19 to determine the best treatment strategy and to minimize the number of infected and isolated individuals through optimal intervention strategies. Calvin Tsay et al. [26] introduced a model to manage the COVID-19 outbreak in the US. It models population dynamics, estimates parameters from data, and employs optimal control strategies to minimize infections via strategic social distancing and testing. Edilson F. Arruda et al. [27] introduced a comprehensive epidemic model addressing multiple viral strains and reinfection due to waning immunity, aiming to balance societal and economic mitigation costs through optimal control. The authors in [28] found an optimal vaccine administration strategy for COVID-19 using real data from China.

In this paper, we study the optimal control system for the SEIRV model of COVID-19 transmission studied by us previously [29], where we implement two control measures, namely vaccination control for susceptible individuals, exposed individuals, and asymptomatic infectious individuals, and quarantine control policies for susceptible individuals. These measures aim to reduce or eliminate the prevalence of COVID-19, while also minimizing the costs associated with vaccination and quarantine.

The rest of the paper is structured as follows. Section 2 presents the basic details of our SEIRV model. Section 3 covers the fundamental concepts of optimal control, utilizing the Filippov–Cesari Existence Theorem and Pontryagin's maximum principle to analyze control strategies and determine the necessary conditions for optimal disease control. Section 3.4 illustrates the mathematical results through numerical simulations. Finally, we summarize our work and propose future research directions.

2. Baseline Model

First, we mention the model that we studied and analyzed in reference [29], which describes the spread of the COVID-19 virus, where the population is subdivided into seven distinct groups: susceptible individuals (S), exposed but not yet infectious individuals (E), vaccinated individuals (V), asymptomatic infectious individuals (I_a), symptomatic and hospitalized infectious individuals (I_s), individuals who have succumbed to the disease (D), and those who have recovered (R).

It is assumed that the total human population N remains constant, implying that birth and death rates are equal. Hence, the normalized reduced system is given by

(1)

$$\begin{cases} S'(t) = \mu - (\alpha_1\eta + \alpha_2(1-\eta))S(t)(I_a(t)+I_s(t)) - \mu S(t) + \lambda_2 V(t) + \gamma R(t) - \lambda_1 S(t), \\ E'(t) = (\alpha_1\eta + \alpha_2(1-\eta))S(t)(I_a(t)+I_s(t)) - (\beta_1+\beta_2+\mu+\lambda_3)E(t), \\ V'(t) = \lambda_1 S(t) + \lambda_3 E(t) + \lambda_4 I_a(t) - (\lambda_2+\lambda_5+\mu)V(t), \\ I_a'(t) = \beta_1 E(t) - (\gamma_1+\lambda_4+\mu)I_a(t), \\ I_s'(t) = \beta_2 E(t) - (\gamma_2+\delta+\mu)I_s(t), \\ R'(t) = \gamma_1 I_a(t) + \gamma_2 I_s(t) + \lambda_5 V(t) - \gamma R(t) - \mu R(t). \end{cases}$$

with initial densities

$$S(0) \geq 0, \quad E(0) \geq 0, \quad V(0) \geq 0, \quad I_a(0) \geq 0, \quad I_s(0) \geq 0, \quad R(0) \geq 0.$$

where α_1 is the infection rate of confined susceptible individuals and α_2 is the infection rate of unconfined susceptible individuals, such that $\alpha_1 < \alpha_2$. Herein, η is the confinement rate within the population, $(\beta_i)_{i=1,2}$ are the exposed-to-infectious rates, γ is the reinfection rate after recovery from a first infection, $(\gamma_i)_{i=1,2}$ are the recovery rates, $(\lambda_i)_{i=1,3,4}$ are the vaccination rates, λ_2 is the rate of vaccine ineffectiveness, λ_5 is the vaccine effectiveness rate, δ is the COVID-19 mortality rate, and μ is the natality rate.

3. Optimal Control Problem

We aim to formulate a control problem for the model system 1 that incorporates vaccination and quarantine as strategic interventions. Our goal is to find an optimal method to utilize vaccination and quarantine to control the spread of the disease and reduce its impact on public health. In the following, we discuss these control interventions in detail.

To ensure that vaccinated individuals benefit from vaccination at minimum cost within a specified period of time, this can be achieved by replacing the constant vaccination rates λ_1, λ_3, and λ_4 in model (1) with the time-dependent control functions $u_1(t)$, $u_2(t)$, and $u_3(t)$, respectively, which act as vaccination controls, where $u_1(t)$ is a control function that represents the percentage of susceptible individuals (S) being vaccinated at each instant of time t, with $t \in [0, t_f]$, $u_2(t)$ is a control function that represents the percentage of exposed individuals (E) being vaccinated at each instant of time t, with $t \in [0, t_f]$, and $u_3(t)$ is a control function that represents the percentage of asymptomatic infectious individuals (I_a) being vaccinated at each instant of time t, with $t \in [0, t_f]$.

Quarantine programs for susceptible individuals (S) are implemented to control the spread of the disease, but they come with significant costs. To minimize these costs, we let η vary with time and replace it with $u_4(t)$ in model (1). Thus, the mathematical system describing the spread of COVID-19 disease with control is given by the following nonlinear differential equations:

$$(2)\quad \begin{cases} S'(t) = \mu - (\alpha_1 u_4(t) + \alpha_2 (1 - u_4(t))) S(t) (I_a(t) + I_s(t)) - \mu S(t) + \lambda_2 V(t) \\ \qquad\quad + \gamma R(t) - u_1(t) S(t), \\ E'(t) = (\alpha_1 u_4(t) + \alpha_2 (1 - u_4(t))) S(t) (I_a(t) + I_s(t)) - (\beta_1 + \beta_2 + \mu + u_2(t)) E(t), \\ V'(t) = u_1(t) S(t) + u_2(t) E(t) + u_3(t) I_a(t) - (\lambda_2 + \lambda_5 + \mu) V(t), \\ I_a'(t) = \beta_1 E(t) - (\gamma_1 + u_3(t) + \mu) I_a(t), \\ I_s'(t) = \beta_2 E(t) - (\gamma_2 + \delta + \mu) I_s(t), \\ R'(t) = \gamma_1 I_a(t) + \gamma_2 I_s(t) + \lambda_5 V(t) - \gamma R(t) - \mu R(t). \end{cases}$$

We define the set of admissible controls Ω_{ad} as

$$\Omega_{ad} = \left\{ u = (u_1, u_2, u_3, u_4) : u_i \text{ are measurable with } 0 \le u_i(t) \le 1,\ i = 1,2,3,4,\ t \in [0, t_f] \right\}.$$

Here, t represents time and t_f represents the final time for the control strategy of the SARS disease.

3.1. Objective function. The target of the considered control strategy is to

- Lower the COVID-19 exposed individuals (E), asymptomatic infectious individuals (I_a), and symptomatic and hospitalized infectious individuals (I_s).
- Minimize the cost of applied controls u_1, u_2, u_3, and u_4.

In achieving these goals, we formulate the objective functional as follows:

(3)
$$J(u(t)) = \int_0^{t_f} \left(m_1 E(t) + m_2 I_a(t) + m_3 I_s(t) + \frac{w_1}{2} u_1^2(t) + \frac{w_2}{2} u_2^2(t) + \frac{w_3}{2} u_3^2(t) + \frac{w_4}{2} u_4^2(t) \right) dt.$$

where m_1 is a weight for the number of exposed infected individuals, m_2 is a weight for the number of asymptomatic infected individuals, m_3 is a weight for the number of symptomatic infected individuals, w_1 is a positive constant representing the weight for the cost of vaccinating the susceptible subpopulation S, w_2 is a positive constant representing the weight for the cost of vaccinating the exposed subpopulation (E), w_3 is a positive constant representing the weight for the cost of vaccinating the asymptomatic infectious subpopulation (I_a), w_4 is a positive constant representing the weight for the cost of quarantining the susceptible subpopulation (S), $m_1 E(t)$ describes the cost related to exposed infected individuals, $m_2 I_a(t)$ describes the cost related to asymptomatic infected individuals, $m_3 I_s(t)$ describes the cost related to symptomatic infected individuals, $\frac{w_1}{2} u_1^2(t)$ represents the total cost of vaccinating the susceptible individuals, $\frac{w_2}{2} u_2^2(t)$ represents the total cost of vaccinating the exposed individuals, $\frac{w_3}{2} u_3^2(t)$ represents the total cost of vaccinating asymptomatic infected individuals, and $\frac{w_4}{2} u_4^2(t)$ represents the total cost of quarantining the susceptible individuals.

Our goal is to find optimal controls $u^* = \left(u_1^*, u_2^*, u_3^*, u_4^*\right)$ such that the corresponding state trajectories solve the system (2) for $t \in [0, t_f]$ and minimize the specified cost functional in (3). That is,

$$J(u^*(t)) = \min \{J(u) : u \in \Omega_{ad}\}. \tag{4}$$

3.2. Existence of an Optimal Control. Before proceeding with the characterization of the optimal control, we first establish the existence of an optimal solution for the control problem.

Theorem 3.1. *The optimal control problem* (2)–(3) *has a solution.*

Proof. To prove the existence of an optimal control u^*, we need to verify the conditions given by Fleming and Rishel [30].

$1-$ The set of all solutions of the control system (2) with associated control functions in Ω_{ad} is nonempty.

$2-$ The admissible control set Ω_{ad} is convex and closed.

$3-$ The right-hand side of the state system is bounded by a linear function of the state and control variables.

$4-$ The integrand

$$L(E,I_a,I_s,u) = m_1E(t)+m_2I_a(t)+m_3I_s(t)+\frac{w_1}{2}u_1^2(t)+\frac{w_2}{2}u_2^2(t)+\frac{w_3}{2}u_3^2(t)+\frac{w_4}{2}u_4^2(t)$$

of the objective functional is convex on Ω_{ad}.

$5-$ There exist constants b_1, b_2, and a constant $\rho > 1$ such that

$$L(x,u) \geq b_2\|u\|^{\rho} - b_1,$$

where $\|u\| = \left(u_1^2+u_2^2+u_3^2+u_4^2\right)^{\frac{1}{2}}$.

• To prove condition 1, we will use a simplified version of an existence result (Boyce and DiPrima) [31]. Let $x = (x_1,x_2,x_3,x_4,x_5,x_6) = (S,E,V,I_a,I_s,R)$. We have

$$x_i' = F_{x_i}(t,x_1,x_2,x_3,x_4,x_5,x_6),$$

where x_1', x_2', x_3', x_4', x_5', and x_6' are given by the right-hand side of the equations of system (2). Let u_1, u_2, u_3, and u_4 be constants, and since all parameters are constants and x_1, x_2, x_3, x_4, x_5, and x_6 are continuous, then

(a) F_S, F_E, F_V, F_{I_a}, F_{I_s}, and F_R are continuous.

(b) The partial derivatives $\dfrac{\partial F_{x_i}}{\partial x_i}$, $i = 1,\ldots,6$, are all continuous.

Therefore, according to [31], there exists a unique solution (S,E,V,I_a,I_s,R) that satisfies the initial conditions. Condition 1 is satisfied.

• To prove condition 2, we take any controls $u = (u_1,u_2,u_3,u_4) \in \Omega_{ad}$ and $v = (v_1,v_2,v_3,v_4) \in \Omega_{ad}$, and we prove that

$$\theta u_i + (1-\theta)v_i \in \Omega_{ad}, \qquad \theta \in [0,1].$$

We have $0 \leq \theta u_i + (1-\theta)v_i$. Additionally, we observe that

$$\begin{cases} \theta u_i \leq \theta, \\ (1-\theta)v_i \leq (1-\theta). \end{cases}$$

Then, we obtain

$$\theta u_i + (1-\theta)v_i \leq \theta + (1-\theta) = 1.$$

Hence, we have

$$0 \leq \theta u_i + (1-\theta)v_i \leq 1, \qquad i = 1,2,3,4.$$

This implies that

$$\theta u_i + (1-\theta)v_i \in \Omega_{ad}, \qquad \theta \in [0,1].$$

Therefore, condition 2 is satisfied.

- To prove condition 3, we have

$$\begin{aligned}
F_S &= S'(t) \leq \mu + \lambda_2 V(t) + \gamma R(t) + (\alpha_2 - \alpha_1) S(t) (I_a(t) + I_s(t)) u_4(t) - u_1(t) S(t), \\
F_E &= E'(t) \leq (\alpha_1 - \alpha_2) S(t) (I_a(t) + I_s(t)) u_4(t) + \alpha_2 S(t) - u_2(t) E(t), \\
F_V &= V'(t) \leq u_1(t) S(t) + u_2(t) E(t) + u_3(t) I_a(t), \\
F_{I_a} &= I_a'(t) \leq \beta_1 E(t) - u_3(t) I_a(t), \\
F_{I_S} &= I_s'(t) \leq \beta_2 E(t), \\
F_R &= R'(t) = \gamma_1 I_a(t) + \gamma_2 I_s(t) + \lambda_5 V(t).
\end{aligned}$$

So, we can rewrite system (2) in matrix form as

$$F(t,S,E,V,I_a,I_s,R) \leq \Lambda + Ax(t) + Bu(t),$$

where

$$\begin{cases} F(t,S,E,V,I_a,I_s,R) = [F_S, F_E, F_V, F_{I_a}, F_{I_s}, F_R]^T, \\ \Lambda = [\mu, 0, 0, 0, 0, 0]^T, \\ x(t) = [S, E, V, I_a, I_s, R]^T, \\ u(t) = [u_1, u_2, u_3, u_4]^T. \end{cases}$$

and

$$A=\begin{pmatrix} 0 & 0 & \lambda_2 & 0 & 0 & \gamma \\ \alpha_2 & 0 & 0 & 0 & 0 & 0 \\ 0 & 0 & 0 & 0 & 0 & 0 \\ 0 & \beta_1 & 0 & 0 & 0 & 0 \\ 0 & \beta_2 & 0 & 0 & 0 & 0 \\ 0 & 0 & \lambda_5 & \gamma_1 & \gamma_2 & 0 \end{pmatrix}, \quad B=\begin{pmatrix} -S & 0 & 0 & (\alpha_2-\alpha_1)S(I_a+I_s) \\ 0 & -E & 0 & (\alpha_1-\alpha_2)S(I_a+I_s) \\ S & E & I_a & 0 \\ 0 & 0 & -I_a & 0 \\ 0 & 0 & 0 & 0 \\ 0 & 0 & 0 & 0 \end{pmatrix}.$$

We have a linear function of state variable and control vector. Therefore, we write

$$\begin{aligned} \|F(t,S,E,V,I_a,I_s,R)\| &\leq \|\Lambda\|+\|A\|\,\|x(t)\|+\|B\|\,\|u(t)\| \\ &\leq \varphi+\psi(\|x(t)\|+\|u(t)\|). \end{aligned}$$

where $\|\Lambda\|\leq\varphi$ and $\psi=\max(\|A\|,\|B\|)$. Thus condition 3 is proved.

- To prove condition 4, we want to prove for any $\theta\in[0,1]$ such that

$$L(t,x,(1-\theta)u+\theta v)\leq(1-\theta)L(t,x,u)+\theta L(t,x,v),$$

where $u=(u_1,u_2,u_3,u_4)\in\Omega_{ad}$ and $v=(v_1,v_2,v_3,v_4)\in\Omega_{ad}$. Here,

$$(1-\theta)L(t,x,v_1)+\theta(t,x,v_2)=m_1E+m_2I_a+m_3I_s+\frac{(1-\theta)}{2}\sum_{i=1}^{4}w_iu_i^2+\frac{\theta}{2}\sum_{i=1}^{4}w_iv_i^2$$

and

$$L(t,x,(1-\theta)u+\theta v)=m_1E+m_2I_a+m_3I_s+\frac{1}{2}\sum_{i=1}^{4}w_1((1-\theta)u_i+\theta v_i)^2.$$

Further, we have

$$\begin{aligned} &(1-\theta)L(t,x,v_1)+\theta(t,x,v_2)-L(t,x,(1-\theta)u+\theta v) \\ =\;& \frac{(1-\theta)}{2}\sum_{i=1}^{4}w_iu_i^2+\frac{\theta}{2}\sum_{i=1}^{4}w_iv_i^2-\frac{1}{2}\sum_{i=1}^{4}w_1((1-\theta)u_i+\theta v_i)^2, \\ =\;& \frac{1}{2}\sum_{i=1}^{4}w_i\left[(1-\theta)u_i^2+\theta v_i^2-((1-\theta)u_i+\theta v_i)^2\right], \\ =\;& \frac{1}{2}\sum_{i=1}^{4}w_i\left(\sqrt{\theta(1-\theta)}u_i-\sqrt{\theta(1-\theta)}v_i\right)^2, \\ =\;& \frac{1}{2}\theta(1-\theta)\sum_{i=1}^{4}w_i(u_i-v_i)^2\geq 0. \end{aligned}$$

Hence, the integrand is convex on Ω_{ad}. Thus condition 4 also holds.

- To prove condition 5, it can be seen that $w_4u_4^2 \leq w_4$, that is, $\frac{w_4}{2}u_4^2 \leq \frac{w_4}{2}$. We have

$$\begin{aligned} L(x,u) &= m_1E + m_2I_a + m_3I_s + \frac{w_1}{2}u_1^2 + \frac{w_2}{2}u_2^2 + \frac{w_3}{2}u_3^2 + \frac{w_4}{2}u_4^2, \\ &\geq \frac{w_1}{2}u_1^2 + \frac{w_2}{2}u_2^2 + \frac{w_3}{2}u_3^2 + \frac{w_4}{2}u_4^2, \\ &\geq \frac{w_1}{2}u_1^2 + \frac{w_2}{2}u_2^2 + \frac{w_3}{2}u_3^2 + \frac{w_4}{2}u_4^2 - \frac{w_4}{2}, \\ &\geq \min\left(\frac{w_1}{2}, \frac{w_2}{2}, \frac{w_3}{2}, \frac{w_4}{2}\right)\|u\|^2 - \frac{w_4}{2}, \end{aligned}$$

where, $\|u\| = \left(u_1^2 + u_2^2 + u_3^2 + u_4^2\right)^{\frac{1}{2}}$. Choosing $b_2 = \min\left(\frac{w_1}{2}, \frac{w_2}{2}, \frac{w_3}{2}, \frac{w_4}{2}\right)$ and $b_1 = \frac{w_4}{2}$, we get $L(x,u) \geq b_2\|u\|^\rho - b_1$. This completes the proof. □

3.3. Characterization of the Optimal Control. In this section, we define the optimal controls $u^* = \left(u_1^*, u_2^*, u_3^*, u_4^*\right)$ that provide the best values for the control measures and the related state variables $(S^*, E^*, V^*, I_a^*, I_s^*, R^*)$. We apply Pontryagin's maximum principle [32] to derive the necessary condition for the optimal control. The adjoint function is utilized to link the system of differential equations (2) to the objective functional (3), resulting in the formation of the Hamiltonian. This method converts the problem into minimizing the Hamiltonian $H(t)$ over time t defined by

$$\begin{aligned} (5) \qquad & H(x(t), u(t), \Lambda(t)) \\ = & \Big(m_1E(t) + m_2I_a(t) + m_3I_s(t) + \frac{w_1}{2}u_1^2(t) + \frac{w_2}{2}u_2^2(t) + \frac{w_3}{2}u_3^2(t) + \frac{w_4}{2}u_4^2(t)\Big) \\ & + \lambda_s[\mu - (\alpha_1u_4(t) + \alpha_2(1 - u_4(t)))S(t)(I_a(t) + I_s(t)) - \mu S(t) + \lambda_2V(t) + \gamma R(t) - u_1S] \\ & + \lambda_E[(\alpha_1u_4(t) + \alpha_2(1 - u_4(t)))S(t)(I_a(t) + I_s(t)) - (\beta_1 + \beta_2 + \mu + u_2(t))E(t)] \\ & + \lambda_v[u_1(t)S(t) + u_2(t)E(t) + u_3(t)I_a(t) - (\lambda_2 + \lambda_5 + \mu)V(t)] \\ & + \lambda_{I_a}[\beta_1E(t) - (\gamma_1 + u_3(t) + \mu)I_a(t)] \\ & + \lambda_{I_S}[\beta_2E(t) - (\gamma_2 + \delta + \mu)I_s(t)] \\ & + \lambda_R[\gamma_1I_a(t) + \gamma_2I_s(t) + \lambda_5V(t) - \gamma R(t) - \mu R(t)], \end{aligned}$$

where $\Lambda = (\lambda_S, \lambda_E, \lambda_V, \lambda_{I_a}, \lambda_{I_s}, \lambda_R)$ are the adjoint variables, and the state variables for the population dynamics are denoted by $x(t) = (S(t), E(t), V(t), I_a(t), I_s(t), R(t))$. That is, λ_S adjoint for $S(t)$, λ_E adjoint for $E(t)$, λ_V adjoint for $V(t)$, λ_{I_a} adjoint for $I_a(t)$, λ_{I_s} adjoint for $I_s(t)$, and λ_R adjoint for $R(t)$.

Theorem 3.2. *For optimal control $u^* = \left(u_1^*, u_2^*, u_3^*, u_4^*\right)$ and the solutions $(S^*, E^*, V^*, I_a^*, I_s^*, R^*)$ of the corresponding state system* (2)*, there exists a continuously differentiable vector*

$$\Lambda(t) = (\lambda_S(t), \lambda_E(t), \lambda_V(t), \lambda_{I_a}(t), \lambda_{I_s}(t), \lambda_R(t))$$

satisfying

$$(6)\quad \begin{cases} \frac{d\lambda_S}{dt} = -\frac{\partial H}{\partial S} = (\lambda_s - \lambda_E)(\alpha_1 u_4 + \alpha_2 (1 - u_4))(I_a + I_s) + (\lambda_s - \lambda_v) u_1 + \lambda_s \mu, \\ \frac{d\lambda_E}{dt} = -\frac{\partial H}{\partial E} = +\lambda_E (\beta_1 + \beta_2 + \mu + u_2) - m_1 - \lambda_v u_2 - \lambda_{I_a} \beta_1 - \lambda_{I_S} \beta_2, \\ \frac{d\lambda_v}{dt} = -\frac{\partial H}{\partial V} = \lambda_v (\lambda_2 + \lambda_5 + \mu) - \lambda_s \lambda_2 - \lambda_R \lambda_5, \\ \frac{d\lambda_{I_a}}{dt} = -\frac{\partial H}{\partial I_a} = (\lambda_s - \lambda_E)(\alpha_1 u_4 + \alpha_2 (1 - u_4)) S + \lambda_{I_a} (\gamma_1 + u_3 + \mu) - m_2 - \lambda_v u_3 - \lambda_R \gamma_1, \\ \frac{d\lambda_{I_s}}{dt} = -\frac{\partial H}{\partial I_s} = (\lambda_s - \lambda_E)(\alpha_1 u_4 + \alpha_2 (1 - u_4)) S + \lambda_{I_S} (\gamma_2 + \delta + \mu) - m_3 - \lambda_R \gamma_2, \\ \frac{d\lambda_R}{dt} = -\frac{\partial H}{\partial R} = \lambda_R (\gamma + \mu) - \lambda_s \gamma. \end{cases}$$

with the transversality conditions

$$(7)\quad \lambda_S\left(t_f\right) = \lambda_E\left(t_f\right) = \lambda_V\left(t_f\right) = \lambda_{I_a}\left(t_f\right) = \lambda_{I_s}\left(t_f\right) = \lambda_R\left(t_f\right) = 0$$

and optimal controls

$$(8)\quad \begin{cases} u_1^* = \min\left(1, \max\left(0, \frac{(\lambda_s - \lambda_v)}{w_1} S\right)\right), \\ u_2^* = \min\left(1, \max\left(0, \frac{(\lambda_E - \lambda_v)}{w_2} E\right)\right), \\ u_3^* = \min\left(1, \max\left(0, \frac{(\lambda_{I_a} - \lambda_v)}{w_3} I_a\right)\right), \\ u_4^* = \min\left(1, \max\left(0, \frac{(\alpha_2 - \alpha_1)(\lambda_E - \lambda_s)}{w_4} S(I_a + I_s)\right)\right). \end{cases}$$

Proof. By deriving the Hamiltonian equation (5) with respect to $S(t)$, $E(t)$, $V(t)$, $I_a(t)$, $I_s(t)$, and $R(t)$, we obtain

$$(9)\quad \begin{cases} \frac{d\lambda_S}{dt} = -\frac{\partial H}{\partial S} = (\lambda_s - \lambda_E)(\alpha_1 u_4 + \alpha_2 (1 - u_4))(I_a + I_s) + (\lambda_s - \lambda_v) u_1 + \lambda_s \mu, \\ \frac{d\lambda_E}{dt} = -\frac{\partial H}{\partial E} = +\lambda_E (\beta_1 + \beta_2 + \mu + u_2) - m_1 - \lambda_v u_2 - \lambda_{I_a} \beta_1 - \lambda_{I_S} \beta_2, \\ \frac{d\lambda_v}{dt} = -\frac{\partial H}{\partial V} = \lambda_v (\lambda_2 + \lambda_5 + \mu) - \lambda_s \lambda_2 - \lambda_R \lambda_5, \\ \frac{d\lambda_{I_a}}{dt} = -\frac{\partial H}{\partial I_a} = (\lambda_s - \lambda_E)(\alpha_1 u_4 + \alpha_2 (1 - u_4)) S + \lambda_{I_a} (\gamma_1 + u_3 + \mu) - m_2 - \lambda_v u_3 - \lambda_R \gamma_1, \\ \frac{d\lambda_{I_s}}{dt} = -\frac{\partial H}{\partial I_s} = (\lambda_s - \lambda_E)(\alpha_1 u_4 + \alpha_2 (1 - u_4)) S + \lambda_{I_S} (\gamma_2 + \delta + \mu) - m_3 - \lambda_R \gamma_2, \\ \frac{d\lambda_R}{dt} = -\frac{\partial H}{\partial R} = \lambda_R (\gamma + \mu) - \lambda_s \gamma. \end{cases}$$

□

To obtain the optimality condition (4), we differentiate the Hamiltonian function with respect to u_1^*, u_2^*, u_3^*, and u_4^*, such that

$$\frac{\partial H}{\partial u_m} = 0, \quad m = 1,2,3,4.$$

That is

$$\text{(10)} \qquad \begin{cases} \frac{\partial H}{\partial u_1} = w_1 u_1 + (\lambda_v - \lambda_s)\, S = 0, \\ \frac{\partial H}{\partial u_2} = w_2 u_2 + (\lambda_v - \lambda_E)\, E = 0, \\ \frac{\partial H}{\partial u_3} = w_3 u_3 + (\lambda_v - \lambda_{I_a})\, I_a = 0, \\ \frac{\partial H}{\partial u_4} = w_4 u_4 + (\alpha_1 - \alpha_2)\, S\,(I_a + I_s)\,(\lambda_E - \lambda_s) = 0. \end{cases}$$

Solving for the optimal controls yields

$$\text{(11)} \qquad \begin{cases} u_1^* = \frac{(\lambda_s - \lambda_v)}{w_1} S, \\ u_2^* = \frac{(\lambda_E - \lambda_v)}{w_2} E, \\ u_3^* = \frac{(\lambda_{I_a} - \lambda_v)}{w_3} I_a, \\ u_4^* = \frac{(\alpha_2 - \alpha_1)(\lambda_E - \lambda_s)}{w_4} S\,(I_a + I_s)\,. \end{cases}$$

From the boundedness of $u_i^*(t)$ on $[0,1]$ and the minimality condition, it yields

$$u_1^*(t) = \begin{cases} 0, & \text{if } \dfrac{\partial H}{\partial u_1} > 0, \\ \dfrac{(\lambda_s - \lambda_v)}{w_1} S, & \text{if } \dfrac{\partial H}{\partial u_1} = 0, \\ 1, & \text{if } \dfrac{\partial H}{\partial u_1} < 0, \end{cases} \quad u_2^*(t) = \begin{cases} 0, & \text{if } \dfrac{\partial H}{\partial u_2} > 0, \\ \dfrac{(\lambda_E - \lambda_v)}{w_2} E, & \text{if } \dfrac{\partial H}{\partial u_2} = 0, \\ 1, & \text{if } \dfrac{\partial H}{\partial u_2} < 0, \end{cases}$$

$$u_3^*(t) = \begin{cases} 0, & \text{if } \dfrac{\partial H}{\partial u_3} > 0, \\ \dfrac{(\lambda_{I_a} - \lambda_v)}{w_3} I_a, & \text{if } \dfrac{\partial H}{\partial u_3} = 0, \\ 1, & \text{if } \dfrac{\partial H}{\partial u_3} < 0, \end{cases}$$

and

$$u_4^*(t) = \begin{cases} 0, & \text{if } \dfrac{\partial H}{\partial u_4} > 0, \\ \dfrac{(\alpha_2 - \alpha_1)(\lambda_E - \lambda_s)}{w_4} S\,(I_a + I_s)\,, & \text{if } \dfrac{\partial H}{\partial u_4} = 0, \\ 1, & \text{if } \dfrac{\partial H}{\partial u_4} < 0. \end{cases}$$

So, it can be written as

$$
\begin{cases}
u_1^* = \min\left(1, \max\left(0, \frac{(\lambda_s - \lambda_v)}{w_1} S\right)\right), \\
u_2^* = \min\left(1, \max\left(0, \frac{(\lambda_E - \lambda_v)}{w_2} E\right)\right), \\
u_3^* = \min\left(1, \max\left(0, \frac{(\lambda_{I_a} - \lambda_v)}{w_3} I_a\right)\right), \\
u_4^* = \min\left(1, \max\left(0, \frac{(\alpha_2 - \alpha_1)(\lambda_E - \lambda_s)}{w_4} S\left(I_a + I_s\right)\right)\right).
\end{cases} \tag{12}
$$

The proof is completed.

3.4. Simulation numérique. In this section, numerical simulations are performed for systems (2) and (3) using the forward–backward sweep method [33] in MATLAB to examine the impact of control policy strategies on disease dynamics and the related implementation costs, with specific initial and parameter values given for the simulations in Table 3.4.

TABLE 1. Initial values and parameter values.

Parameter values	N	μ	γ	λ_2	λ_5	δ
Estimation	100000	5.644e-4(per day)	0.0099	0.001765	0.008	0.0055
Parameter values	α_1	α_2	β_1	β_2	γ_1	γ_2
Estimation	0.03	0.12	0.092	0.05	0.01	0.0005
Initial values	$S(0)$	$E(0)$	$V(0)$	$I_a(0)$	$I_s(0)$	$R(0)$
Estimation	0.8	0.05	0.10	0.033	0.016	0.001

In order to explore and analyze the influences of control policy and strategies, we considered the following cases:

- **Strategy** A **(without control):** $u_1 = 0$, $u_2 = 0$, $u_3 = 0$, $u_4 = 0$.
- **Strategy** B**:** $u_1 = 0$, $u_2 = 0$, $u_3 = 0$, $u_4 \neq 0$.
- **Strategy** C**:** $u_1 \neq 0$, $u_2 = 0$, $u_3 = 0$, $u_4 = 0$.
- **Strategy** D**:** $u_1 = 0$, $u_2 \neq 0$, $u_3 = 0$, $u_4 = 0$.
- **Strategy** E**:** $u_1 = 0$, $u_2 = 0$, $u_3 \neq 0$, $u_4 = 0$.

- **Strategy F (combination of u_1 and u_4):** $u_1 \neq 0$, $u_2 = 0$, $u_3 = 0$, $u_4 \neq 0$.
- **Strategy G (combination of u_2 and u_4):** $u_1 = 0$, $u_2 \neq 0$, $u_3 = 0$, $u_4 \neq 0$.
- **Strategy H (using all controls):** $u_1 \neq 0$, $u_2 \neq 0$, $u_3 \neq 0$, $u_4 \neq 0$.

We used parameter values given in Table 3.4 and $w_1 = 250$, $w_2 = 250$, $w_3 = 250$ [34], $w_4 = 10$ [35], and $m_1 = m_2 = m_3 = 1$ for numerical illustration.

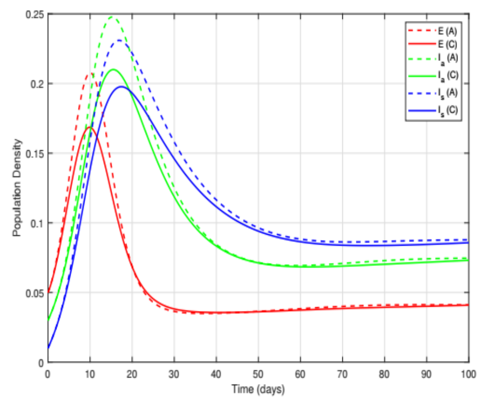

FIGURE 1. Density of Subpopulation (E),(I_a),(I_S) with Control Strategy A, C.

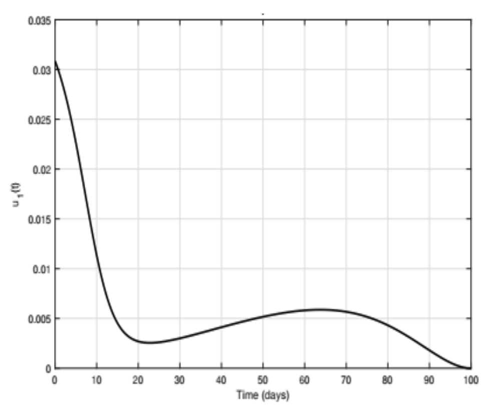

FIGURE 2. Applied control profile u_1.

In Figure (2), the optimal control effort u_1 decreases from its maximum to its minimum value over time, ending after 100 days, indicating that vaccination is no longer needed afterward.

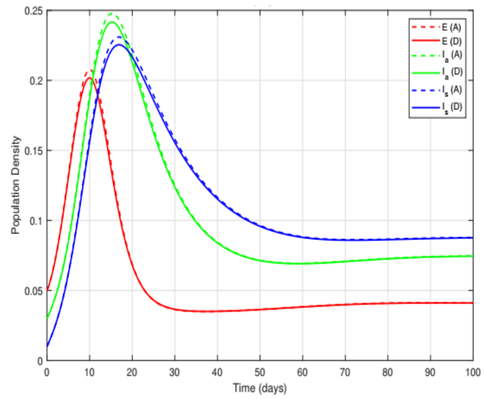

FIGURE 3. Density of Subpopulation (E),(I_a),(I_S) with Control Strategy A, D.

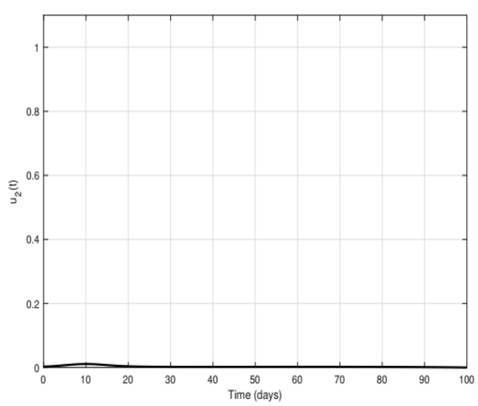

FIGURE 4. Applied control profile u_2.

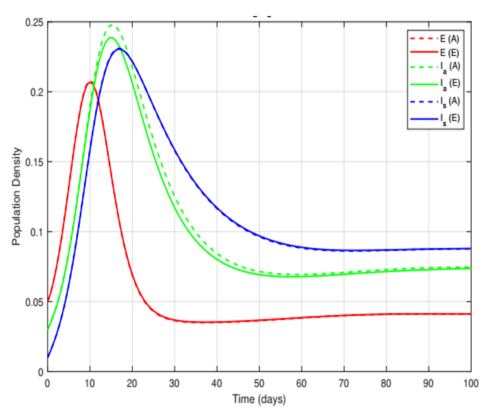

FIGURE 5. Density of Subpopulation (E),(I_a),(I_S) with Control Strategy A, E.

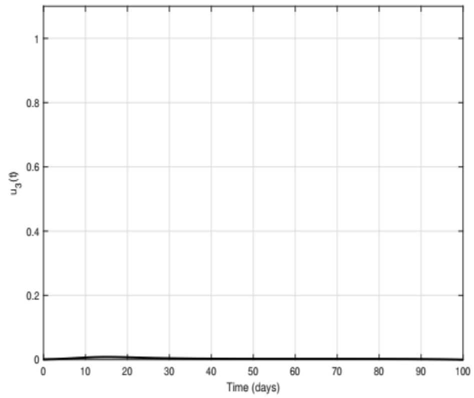

FIGURE 6. Applied control profile u_3.

In Figures (4) and (6), the control efforts u_2 and u_3 are essentially negligible, indicating that vaccinating exposed individuals and asymptomatic infectious individuals is unnecessary.

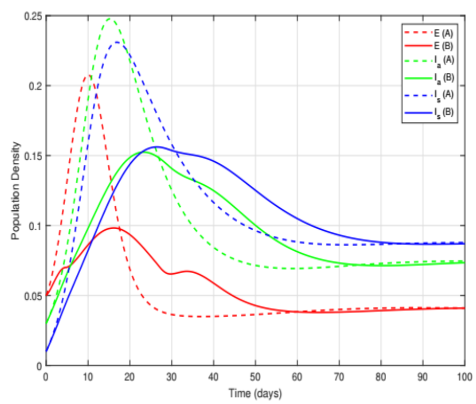

FIGURE 7. Density of Subpopulation (E),(I_a),(I_S) with Control Strategy A, B.

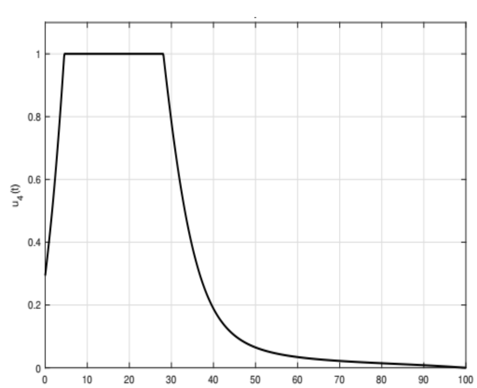

FIGURE 8. Applied control profile u_4.

In Figure (8), the control profile u_4 indicates that quarantine for susceptible individuals should be maintained optimally during the intervention, then gradually reduced after approximately 28 days.

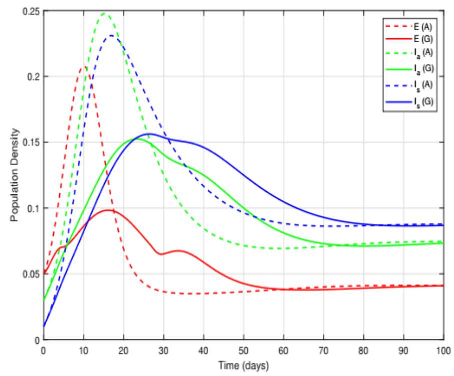

FIGURE 9. Density of Subpopulation (E),(I_a),(I_S) with Control Strategy A, G.

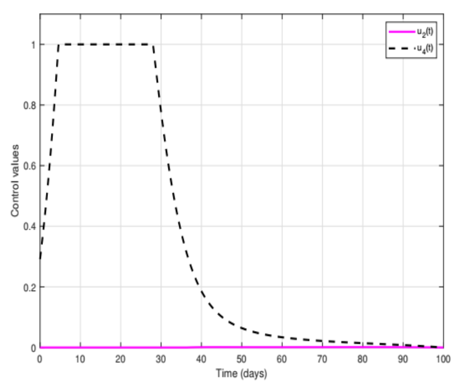

FIGURE 10. Applied control profile $((u_2, u_4))$.

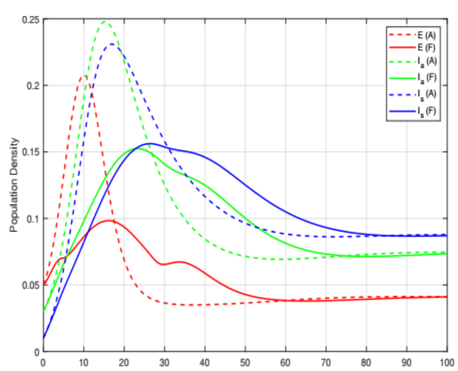

FIGURE 11. Density of Subpopulation (E),(I_a),(I_S) with Control Strategy A, F.

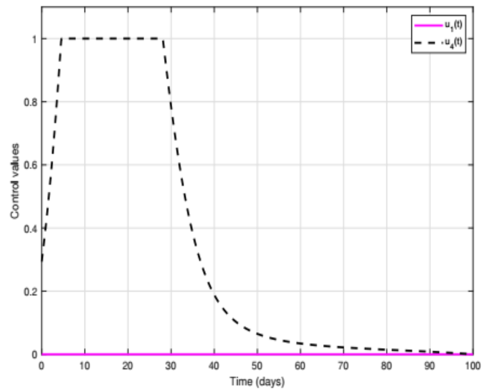

FIGURE 12. Applied control profile $((u_1, u_4))$.

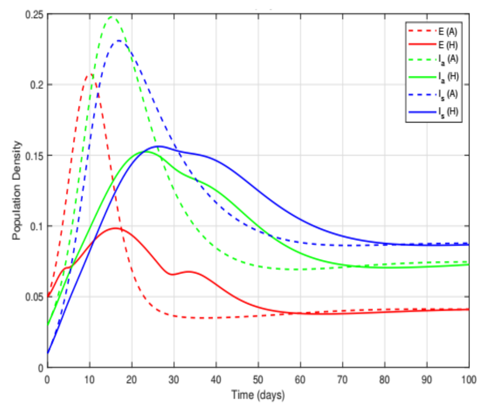

FIGURE 13. Density of Subpopulation (E),(I_a),(I_S) with Control Strategy A, H.

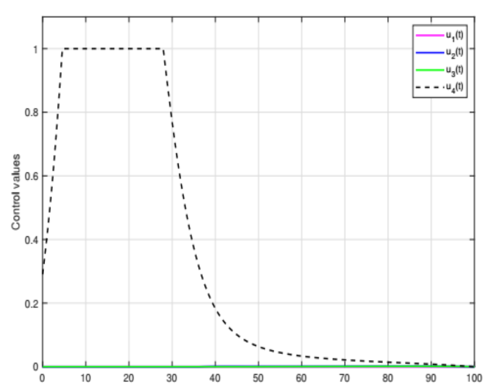

FIGURE 14. Applied control profile $((u_1, u_2, u_3, u_4))$.

In Figures (10), (12), and (14), the combined effects of controls (u_2, u_4), (u_2, u_4), and (u_1, u_2, u_3, u_4) are illustrated. When implemented together, one notes that COVID-19 prevention (control u_4), i.e., quarantine measures, should be implemented optimally and start decreasing after about 28 days throughout the intervention period. Meanwhile, it is observed that the use of the vaccine is not necessary.

Figures (1), (3), (5), (7), (9), (11), and (13) demonstrate how control strategies A, B, C, D, E, F, G, and H influence the dynamics of COVID-19 in the community. We observed that the applied control strategies A, B, C, D, E, F, G, and H cause the exposed population (E), asymptomatic infectious individuals (I_a), and symptomatic and hospitalized infectious individuals (I_s) to show a slight increase under the implementation of control compared to the scenario without control. In other words, the peak levels reached under control are significantly lower than those observed in the absence of control. This indicates that the application of control effectively mitigates the initial surge in cases. Then, the number of individuals (I_a), (I_s), and (E) gradually decreases until each case reaches the stability threshold.

Moreover, each control strategy produces unique peaks in timing and magnitude, highlighting that their effectiveness depends on intensity and duration, and emphasizing the need to choose an optimal approach that balances impact and costs.

4. Conclusion

This study develops optimal control strategies to reduce disease burden and costs, establishing their existence and uniqueness. Using Pontryagin's Minimum Principle, the optimal trajectories are analytically characterized. Numerical simulations demonstrate the effectiveness of these strategies in preventing disease spread within communities. The simulation results show that quarantine and vaccinating susceptible individuals are essential to control COVID-19 spread. Without vaccination, quarantine effectively limits transmission. When both are used together, the impact of quarantine is more significant, making vaccination less critical. This indicates that quarantine alone may suffice to manage COVID-19 in combined intervention strategies.

Conflict of Interests

The authors declare that there is no conflict of interests.

References

[1] N.R. Anakira, A. Almalki, D. Katatbeh, G.B. Hani, A.F. Jameel, K.S. Al Kalbani, M. Abu-Dawas, An Algorithm for Solving Linear and Non-Linear Volterra Integro-Differential Equations, Int. J. Adv. Soft Comput. Appl. 15 (2023), 70–83.

[2] G. Farraj, B. Maayah, R. Khalil, W. Beghami, An Algorithm for Solving Fractional Differential Equations Using Conformable Optimized Decomposition Method, Int. J. Adv. Soft Comput. Appl. 15 (2023), 187–196.

[3] M. Berir, Analysis of the Effect of White Noise on the Halvorsen System of Variable-Order Fractional Derivatives Using a Novel Numerical Method, Int. J. Adv. Soft Comput. Appl. 16 (2024), 294–306.

[4] K.M. Dharmalingam, N. Jeeva, N. Ali, R.K. Al-Hamido, S.E. Fadugba, K. Malesela, F.T. Tolasa, H.S. El-Bahkiry, M. Qousini, Mathematical Analysis of Zika Virus Transmission: Exploring Semi-Analytical Solutions and Effective Controls, Commun. Math. Biol. Neurosci. 2024 (2024), 112. https://doi.org/10.28919/cmbn/8719.

[5] I.M. Bathiha, I. Bendib, A. Ouannas, P. Agarwal, N. Anakira, et al., Finite-Time Synchronization in a Novel Discrete Fractional SIR Model for COVID-19, Bol. Soc. Parana. Mat. 43 (2025), 1–15. https://doi.org/10.5269/bspm.75295.

[6] I.M. Batiha, R. El-Khazali, O.Y. Ababneh, A. Ouannas, R.M. Batyha, S. Momani, Optimal Design of $PI^{\rho}D^{\mu}$-Controller for Artificial Ventilation Systems for Covid-19 Patients, AIMS Math. 8 (2023), 657–675. https://doi.org/10.3934/math.2023031.

[7] I.M. Batiha, N. Djenina, A. Ouannas, T.E. Oussaeif, Fractional-Order SEIR Covid-19 Model: Discretization and Stability Analysis, in: D. Zeidan, J.C. Cortés, A. Burqan, A. Qazza, J. Merker, G. Gharib, (eds) Mathematics and Computation, IACMC 2022. Springer Proceedings in Mathematics & Statistics, Vol 418, Springer, Singapore, (2023). https://doi.org/10.1007/978-981-99-0447-1_20.

[8] M. Almuzini, I.M. Batiha, S. Momani, A Study of Fractional-Order Monkeypox Mathematical Model with Its Stability Analysis, in: 2023 International Conference on Fractional Differentiation and Its Applications (ICFDA), IEEE, 2023, pp. 1-6. https://doi.org/10.1109/icfda58234.2023.10153214.

[9] I.M. Batiha, A. Bouchenak, M. Almuzini, O. Ogilat, N. Anakira, et al., Mathematical Modeling of Human–Rodent Monkeypox Infectious Disease Using a Hierarchical Approach, Commun. Math. Biol. Neurosci. 2025 (2025), 135. https://doi.org/10.28919/cmbn/9583.

[10] I.M. Batiha, H.O. Al-Khawaldeh, M. Almuzini, W.G. Alshanti, N. Anakira, A. Amourah, A Fractional Mathematical Examination on Breast Cancer Progression for the Healthcare System of Jordan, Commun. Math. Biol. Neurosci. 2025 (2025), 29. https://doi.org/10.28919/cmbn/9138.

[11] I.M. Batiha, S. Alshorm, M. Almuzini, Solving Fractional-Order Monkeypox Model by New Numircal Methods. In: Burqan, A., et al. Mathematical Analysis and Numerical Methods. IACMC 2023. Springer Proceedings in Mathematics & Statistics, Vol 466. Springer, Singapore, (2024). https://doi.org/10.1007/978-981-97-4876-1_38.

[12] A.E. Gorbalenya, S.C. Baker, R.S. Baric, R.J. de Groot, C. Drosten, et al., Severe Acute Respiratory Syndrome-Related Coronavirus: The Species and Its Viruses – A Statement of the Coronavirus Study Group, bioRxiv (2020). https://doi.org/10.1101/2020.02.07.937862.

[13] World Health Organization, Weekly Epidemiological Update on COVID-19 - 22 March 2022. https://www.who.int/publications/m/item/weekly-epidemiological-update-on-covid-19---22-march-2022.

[14] Z. Wu, J.M. McGoogan, Characteristics of and Important Lessons from the Coronavirus Disease 2019 (COVID-19) Outbreak in China, JAMA 323 (2020), 1239–1242. https://doi.org/10.1001/jama.2020.2648.

[15] Z.S. Kifle, L. Lemecha Obsu, Optimal Control Analysis of a COVID-19 Model, Appl. Math. Sci. Eng. 31 (2023), 2173188. https://doi.org/10.1080/27690911.2023.2173188.

[16] R.H. Dodd, K. Pickles, B. Nickel, E. Cvejic, J. Ayre, et al., Concerns and Motivations About COVID-19 Vaccination, Lancet Infect. Dis. 21 (2021), 161–163. https://doi.org/10.1016/s1473-3099(20)30926-9.

[17] J. Wang, Y. Peng, H. Xu, Z. Cui, R.O. Williams, The COVID-19 Vaccine Race: Challenges and Opportunities in Vaccine Formulation, AAPS PharmSciTech 21 (2020), 225. https://doi.org/10.1208/s12249-020-01744-7.

[18] P. Zhai, Y. Ding, X. Wu, J. Long, Y. Zhong, et al., The Epidemiology, Diagnosis and Treatment of COVID-19, Int. J. Antimicrob. Agents 55 (2020), 105955. https://doi.org/10.1016/j.ijantimicag.2020.105955.

[19] W. Wei, D. Zheng, Y. Lei, S. Wu, V. Verma, et al., Radiotherapy Workflow and Protection Procedures during the Coronavirus Disease 2019 (COVID-19) Outbreak: Experience of the Hubei Cancer Hospital in Wuhan, China, Radiother. Oncol. 148 (2020), 203–210. https://doi.org/10.1016/j.radonc.2020.03.029.

[20] S. Flaxman, S. Mishra, A. Gandy, H.J.T. Unwin, H. Coupland, et al. Estimating the Number of Infections and the Impact of Non-Pharmaceutical Interventions on COVID-19 in European Countries: Technical Description Update, arXiv:2004.11342 (2020). https://doi.org/10.48550/arXiv.2004.11342.

[21] T. Hamadneh, S.B. Ahmed, H. Al-Tarawneh, O. Alsayyed, G.M. Gharib, et al., The New Four-Dimensional Fractional Chaotic Map with Constant and Variable-Order: Chaos, Control and Synchronization, Mathematics 11 (2023), 4332. https://doi.org/10.3390/math11204332.

[22] L. Lemecha Obsu, S. Feyissa Balcha, Optimal Control Strategies for the Transmission Risk of COVID-19, J. Biol. Dyn. 14 (2020), 590–607. https://doi.org/10.1080/17513758.2020.1788182.

[23] A. Khan, R. Zarin, G. Hussain, N.A. Ahmad, M.H. Mohd, et al., Stability Analysis and Optimal Control of COVID-19 with Convex Incidence Rate in Khyber Pakhtunkhawa (Pakistan), Results Phys. 20 (2021), 103703. https://doi.org/10.1016/j.rinp.2020.103703.

[24] A. Omame, H. Rwezaura, M.L. Diagne, S.C. Inyama, J.M. Tchuenche, COVID-19 and Dengue Co-Infection in Brazil: Optimal Control and Cost-Effectiveness Analysis, Eur. Phys. J. Plus 136 (2021), 1090. https://doi.org/10.1140/epjp/s13360-021-02030-6.

[25] J. Mondal, S. Khajanchi, Mathematical Modeling and Optimal Intervention Strategies of the COVID-19 Outbreak, Nonlinear Dyn. 109 (2022), 177–202. https://doi.org/10.1007/s11071-022-07235-7.

[26] C. Tsay, F. Lejarza, M.A. Stadtherr, M. Baldea, Modeling, State Estimation, and Optimal Control for the US COVID-19 Outbreak, Sci. Rep. 10 (2020), 10711. https://doi.org/10.1038/s41598-020-67459-8.

[27] E.F. Arruda, S.S. Das, C.M. Dias, D.H. Pastore, Modelling and Optimal Control of Multi Strain Epidemics, with Application to COVID-19, PLOS ONE 16 (2021), e0257512. https://doi.org/10.1371/journal.pone.0257512.

[28] G.B. Libotte, F.S. Lobato, G.M. Platt, A.J. Silva Neto, Determination of an Optimal Control Strategy for Vaccine Administration in COVID-19 Pandemic Treatment, Comput. Methods Programs Biomed. 196 (2020), 105664. https://doi.org/10.1016/j.cmpb.2020.105664.

[29] M. Bouziane, A. Mezouaghi, O. Belhamiti, Assessing the Impact of Vaccination Reproduction Number and Endemic Equilibrium on Controlling the Spread of COVID-19: A Sensitivity Analysis, Adv. Math. Sci. Appl. 32 (2023), 399–430.

[30] W.H. Fleming, R.W. Rishel, Deterministic and Stochastic Optimal Control, Springer, New York, 1975. https://doi.org/10.1007/978-1-4612-6380-7.

[31] W.E. Boyce, R.C. DiPrima, D.B. Meade, Elementary Differential Equations and Boundary Value Problems, John Wiley & Sons, (2012).

[32] L.S. Pontryagin, Mathematical Theory of Optimal Processes, CRC Press, (1987).

[33] S. Lenhart, J.T. Workman, Optimal Control Applied to Biological Models, CRC Press, (2007).

[34] A. Rajput, M. Sajid, Tanvi, C. Shekhar, R. Aggarwal, Optimal Control Strategies on COVID-19 Infection to Bolster the Efficacy of Vaccination in India, Sci. Rep. 11 (2021), 20124. https://doi.org/10.1038/s41598-021-99088-0.

[35] J.K.K. Asamoah, M.A. Owusu, Z. Jin, F.T. Oduro, A. Abidemi, et al., Global Stability and Cost-Effectiveness Analysis of COVID-19 Considering the Impact of the Environment: Using Data from Ghana, Chaos Solitons Fractals 140 (2020), 110103. https://doi.org/10.1016/j.chaos.2020.110103.